Electron Beam Optical Characterization via Quantum Coherent Magnetometry

Nicolas DeStefano,[1,1] Saeed Pegahan,[1] Irina Novikova,[1] Eugeniy Mikhailov,[1] Seth Aubin,[1] Todd Averett,[1] Alexandre Camsonne,[2] Gunn Park,[2] Shukui Zhang,[2] Aneesh Ramaswamy,[3] and Svetlana Malinovskaya[3]

[1)]*Dept. of Physics, William & Mary, Williamsburg, VA 23187*

[2)]*Thomas Jefferson National Accelerator Facility, Newport News, VA 23606*

[3)]*Stevens Institude of Technology, Hoboken, NJ 07030*

(Dated: 2 August 2024)

We present a quantum optics-based detection method for determining the position and current of an electron beam by passing it through a dilute vapor of rubidium atoms. The perturbation of the atomic spin's quantum state by the magnetic field created by the moving electrons is then detected optically by monitoring the polarization rotation of a laser resonant with an optical transition of the atoms. By measuring the polarization rotation angle across the laser beam, we recreate a 2D projection of the *e*-beam magnetic field and use it to determine its position, size and total current. We successfully tested this method for an e^- beam with currents ranging from 30 to 110 μA. We also varied the electron energies between 10 to 20 keV and confirmed that our approach is insensitive to it. In principle, this technique holds promise to provide non-invasive characterization of charged particle beams used in accelerators in particle and nuclear physics research.

With the advent of charged particle accelerators came the need for accurate beam diagnostics. As the precision of accelerator-based experiments continues to improve, so must the quality and control of the charged particle beam. The sensitivity and precision of in-situ diagnostics must meet the needs of new particle accelerators where increasingly strict demands are placed on beam spatial properties such as energy, current, emittance and others. Harp Scanners are a gold standard for precise beam precision and profile monitoring but are invasive and must be operated at a low beam current where the beam properties may be different that the production beam. Driven by the need for increasingly precise beam diagnostics in wider range of parameters, relentless efforts continue towards the development of more robust, noninvasive spatial beam parameter measurements. Much of the focus in this development are methods when light or optical signals are employed. Synchrotron radiation has been used for monitoring beam position and size[1–3], and laserwires[4,5] rely on Compton scattering or photo-ionization from a high-power laser to extract the charged particle beam parameters. However, these types of optical diagnostics are limited by practical requirements on the particle and laser beams. For example, synchrotron radiation is only available in particle trajectorybending components such as magnets, while the laserwire method requires a high-intensity laser to slowly scan the beam profile, and often requires additional radiation or electronic detectors. Beam profile monitors based on gas ionization and excitation by particle beams have been demonstrated and used at different accelerators[6–8]. More recently, a 2D beam monitor measuring fluorescence from the interaction between a 5 keV particle beam and a supersonic gas curtain was reported[9], but it is not suitable for longitudinal profile measurement, and the sensitivity is quite limited. It is worth mentioning another type of device widely used in the accelerator community, the RF-based beam monitor, which can provide beam centroid at high resolution, but is incapable of profile measurement[10].

In this paper, we propose a qualitatively different approach to beam diagnostics that takes advantage of recent advances in quantum atom-based optical sensors to map the magnetic field produced by the moving charged particles and then reconstruct the beam parameters. In this proof-of-principle demonstration, we use coupling between resonant laser light and atomic spins to monitor evolution of the latter in the magnetic field of a collimated electron beam. The essence of the proposed approach is shown in Fig. 1(a). The *e*-beam travels through a cell containing a very dilute gas of rubidium atoms. Within the cell each Rb spin precesses at a rate determined by the local magnetic field. A linearly polarized laser beam traverses the volume surrounding the charge particle beam and probes the atomic spins: the nonlinear magnetooptical polarization rotation (NMOR) effect[11–13] rotates the linear polarization axis due the magnetic field of the *e*-beam. By measuring the polarization rotation variation across the laser beam cross-section, we are able to determine the local magnetic field of the *e*-beam and reconstruct its transverse spatial profile. Our detection scheme is non-invasive as the *e*-beam is largely unaffected by low-density alkali vapor (10^{10} –10^{12} cm^{-3})[14]. The strong resonant coupling between laser light and spin quantum coherence strongly enhances the sensitivity compared to methods based on incoherent electron impact-induced fluorescence[9]. This first demonstration is a stepping stone toward more sensitive and

[1] Electronic mail: ncdestefano@wm.edu

comprehensive detection of charged particle beams using advanced spectroscopy techniques.

Our quantum *e*-beam detector relies on two effects: high sensitivity of quantum atomic spin superposition to the magnetic field and strong dependence of atoms' resonant optical properties on their spin state. Thanks to the Zeeman effect, the energy sub-levels with different magnetic quantum numbers, m, shift by different amounts, a superposition of two such sublevels evolves in time, developing a magnetic field dependent relative phase. A resonant, and linearly polarized laser field,

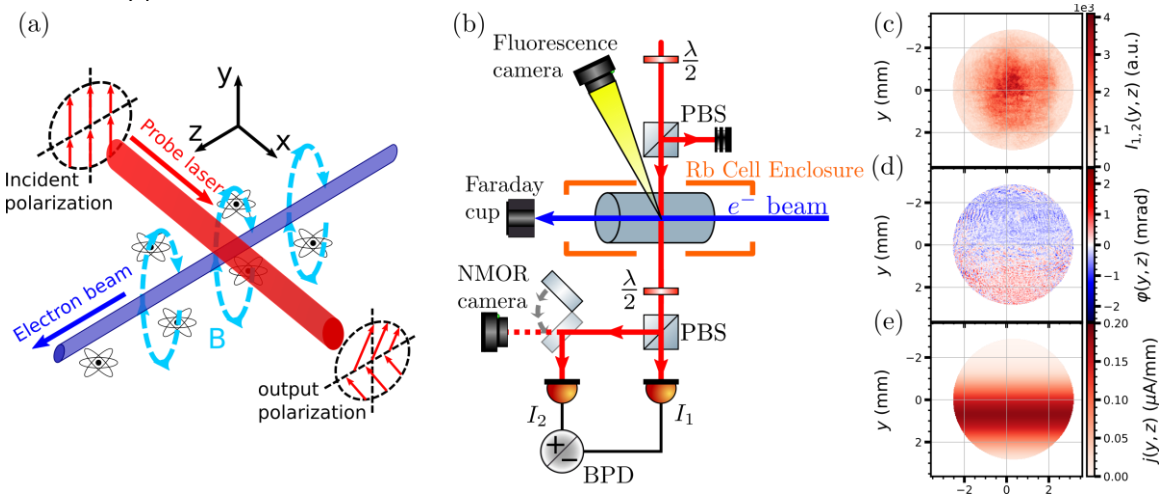

FIG. 1. (a) The basic concept of the charged particle beam detection method. A linear polarization direction of a laser beam (red) is affected by the magnetic field (dashed light blue circles) of an electron beam (dark blue) mediated by the spin coherence of Rb atoms. (b) Schematic of the experimental setup (see text for abbreviations), where a flipper mirror determines BPD- or CCD-based detection. (c) Laser intensity profile at the output of the PBS, recorded by the CCD. (d) The *e*-beam-induced polarization rotation angle, $\varphi(y,z)$, calculated using Eq.(2). (e) The electron current density distribution reconstructed from the erf-function fit of the normalized polarization rotation. For all the image analysis an intensity mask is applied to eliminate data points with laser intensity below 5% of the peak value to prevent infinities during the normalization of the rotation signal in (d).

can simultaneously prepare the desired quantum superposition and measure its evolution. Indeed, the two circularlypolarized components create two-photon links between the states with $\Delta m = \pm 2$ (spin alignment, see Fig. S1 in Supplementary). Its evolution in the magnetic field changes the relative phase between the two circular polarization components, resulting in rotation of the original linear polarization. This effect, called nonlinear magneto-optical polarization rotation (NMOR), is a convenient and sensitive method for optical magnetic field measurements. In the case of long spin coherence lifetime and exact optical resonance, the rate at which the polarization rotation angle ϕ rotates (as the laser propagates along the x-axis) is proportional to the local magnetic field B (see Supplementary A for derivation):

$$\left.\frac{d\varphi}{dx}\right|_{B\approx 0} = \frac{\hbar c N}{I}\gamma\frac{\lambda}{2}, \quad (1)$$

where we assume the greatest contribution to ϕ is when the probe beam direction and magnetic field B are along the $x$axis; λ, I, and c are the wavelength, intensity, and speed of the probe laser light, respectively; N is the density of the Rb vapor, and γ = 5 Hz/nT is the gyromagnetic ratio for ^{85}Rb atoms. In principle, since the intrinsic spin coherence lifetime is very long, and in some experiments[15] was extended up to many seconds, NMOR-based magnetometers can achieve an impressive sub-pT sensitivity[16,17]. When the spin decoherence and optical losses are accounted for, the exact proportionality coefficient between the polarization rotation rate and the applied magnetic field is more complex and depends at some extent on many experimental parameters (lifetimes of both optical spin states, laser frequency detuning from the optical resonance, influence of additional near-resonant atomic levels, etc. See Supplementary Material for detailed derivations). In our experiment, we chose to measure this quantity directly, defining β as $\frac{d}{dx}\phi(y,z)=\beta(y,z)B$ for each point of the laser beam cross-section by applying constant magnetic field and measuring the polarization rotation for each camera pixel. As a result we obtain a rotation response profile $\beta(y,z)$ across the Gaussian laser beam.

In the experiment, the laser beam propagates along the $x$axis, nearly perpendicular to the electron beam direction, designated as the z-direction, and is linearly polarized in the $y$direction, so it is orthogonal to both the electron and the laser beam propagation directions. In this configuration, the laser polarization rotation is only sensitive to the longitudinal

magnetic field component B_x (Faraday configuration)[18]. The magnitude and sign of the rotation angle will depend on the cumulative magnetic field along the optical propagation path. Thus,
by imaging a 2D map of the polarization angle on a camera, we can in principle obtain a transverse profile of the *e*-beam.

The schematic of the experimental setup is shown in Fig. 1(b). We used a commercial thermionic electron source producing a collimated electron beam with energy 10-20 keV and current up to 200 μA. The beam passes through a glass cell containing rubidium vapor before terminating in a Faraday cup. Differential pumping through 8 mm apertures, upand down-stream of the cell, are used to confine the vapor to the cell and to keep it at constant pressure. The vapor was maintained at $\sim 60^\circ$C, corresponding to a ^{85}Rb vapor density of 2.7×10^{11}cm^{-3} and a pressure of $10^{-6}-10^{-5}$ Torr. Since such system is most sensitive to small magnetic fields, we suppress environmental fields by placing the atomic vapor inside a layer of μ-metal magnetic shielding, and use external coils to further reduce the background magnetic fields.

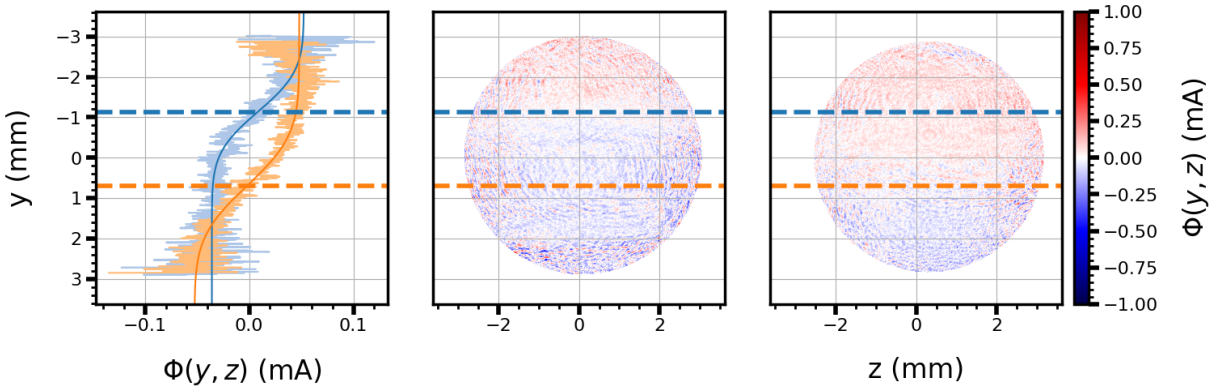

FIG. 2. Measured normalized rotation images for two different electron beam positions. The location of the *e*-beam center is each case is clearly detectable by the reversal of polarization rotation direction. The left panel shows the vertical profiles of the images with the corresponding error function fits, and the horizontal dashed lines indicate the positions of the electron beam center, extracted from the fits.

For optical detection, we use an external cavity diode laser (ECDL) operating at the D_2 line of ^{85}Rb (wavelength λ = 780 nm), specifically at the $5^2S_{1/2},F = 3 \rightarrow 5^2P_{3/2},F'$ transition. The laser beam was linearly polarized using a polarizing beam splitter (PBS) cube and enlarged to 6 mm before the entering the Rb-filled glass cell to capture the full *e*-beam diameter. After the cell, the laser polarization rotation is analyzed using a balanced polarimeter, consisting of a half-wave plate that rotates the polarization by 45°, an analyzer PBS and a differential amplified photodetector. In the absence of the *e*beam, the intensities of the two PBS outputs $I_{1,2}$ are balanced. A small rotation of the polarization ϕ produces a proportional variation between the two channel intensities, allowing accurate calculations of ϕ:

$$\left(\frac{I_2 - I_1}{I}\right) \approx \frac{I_2 - I}{I} \quad 1 \quad \phi$$

$$\arcsin\frac{2(I_2 - I_1)}{2(I_2 + I_1)} \quad (2)$$

In our experiment we measure total power changes in each channel that let us measure the integrated rotation signal, which is convenient for system alignment. For most presented data we use a CCD-based imaging system (magnification 0.50) to record the spatial distribution $\phi(y,z)$ across the laser beam. To ensure the consistency between the recorded intensity masks $I_{1,2}$ they are recorded consecutively at the same camera position, but with different angle of the wavepate before the polarizer. An example of such intensity profile for one of the channels is shown in Fig. 1(c), in which the intensity difference between two channels, induced by the *e*-beam, is not distinguishable by a naked eye. Because the laser beam has Gaussian intensity profile, we only use its central part with sufficient intensity in further calculations. In addition, we pulse the electron beam was pulsed on and off at 1Hz to record two consecutive images, with and without the *e*-beam. Subtracting them from each other allows us to remove any residual polarization rotation due to stray magnetic fields or optical elements to ensure that we only detect the polarization rotation caused by the *e*-beam.

By capturing the intensity profiles of the two outputs on a CCD camera with two waveplate positions, we were able to calculate local variations of $\phi(y,z)$ within the laser beam cross-section as shown in Fig. 1(d). The angle distribution within the laser beam is extracted by applying Eq. 2 to each camera pixel. Since the *e*-beam generates circulating magnetic field in x–y plane, and the nonlinear polarization rotation is primarily sensitive to the x component of the magnetic field, we expect to see a sign change in the measured polarization rotation angle below and above the center of the *e*-beam, as shown in Fig. 1(a).

To obtain more qualitative information about the *e*-beam, we assume that its current density $j(x,y)$ is cylindrically symmetric and has a Gaussian transverse profile:

$$j(x,y) = I_0 e^{-\frac{x^2}{2w^2}+2y^2}, \qquad (3)$$ πw^2

where I_0 is the total current, and w is the beam $1/e^2$ halfwidth. Corresponding magnetic field maintains cylindrial symmetry, forming concentric field lines around the beam central axis, and its magnitude can be easily found using Ampere's law:

$$B(x,y) = \frac{\mu_0 I_0}{2\pi w^2 \sqrt{x^2+y^2}} \left(1 - e^{-\frac{x^2}{2w^2}+2y^2}\right), \qquad (4)$$

where μ_0 is the permeability of free space.

In the limit of a weak magnetic field, the total measured polarization rotation is integrated along the laser probe propagation path L:

$$\phi(x,y,z) = \beta(y,z) \int_{-L/2}^{L/2} B_x(x,y)\,dx. \qquad (5)$$

Here we assume that the rotation angle is small and that the e-beam is collimated and its magnetic field has no $z$dependence. In this case any changes in the polarization rotation in this direction can only be caused by the variation in the atomic response $\beta(y,z)$ due to, e.g., laser intensity variation. Using Eq. 4, and assuming that the length of the cell is much larger than the e-beam width $L \gg w$, we can find an analytical expression for the polarization rotation for an electron beam centered at vertical location $y = y_0$:

$$\phi(y,z) = \beta(y,z) \frac{\mu_0 I_0 (y - y0)}{2\pi} \int_{-L/2}^{L/2} \frac{1 - e^{-\frac{x^2+(y-y0)^2}{w^2}}}{x^2 + (y - y0)^2} dx$$
$$\approx \beta(y,z) \frac{\mu_0 I_0}{2} \mathrm{erf}((y - y0)/w), \qquad (6)$$

where we assume $\pm\infty$ integration limits, and erf(x) is the error function. It is convenient to introduce a normalized signal —! FixMe ND: Current density generator? !— $\Phi(y,z) = \phi(y,z)/(\mu_0 \beta(y,z))$ since it depends only on the $e$beam current distribution. For a Gaussian current distribution, according to Eq.(6), the normalized signal is an error function, centered at the vertical position of the e-beam y_0, and the maximum variation of $j(y,z)$ depends only on the total e-beam current. That allows for robust measurements of these parameters even for a noisy signals. An example of the electron current distribution using the parameters obtained from the fitting the normalized rotation spectra are shown in Fig. 1(e).

Fig.2 shows the examples of the recorded normalized signal $\Phi(y,z)$ for two positions of the e-beam. As expected, the polarization rotation changes direction from positive to negative at the e-beam center position, and the signal is uniform in the z-direction. To obtain the e-beam parameters we fit the 2D experimental signal distribution with the error function. We then repeated the measurements for varying electron beam positions and values of the total current, as shown in Fig. 3. One of the challenges of this experiment is the absence of reliable independent e-beam diagnostics at the Rb cell. To verify the accuracy of the beam position measurement we captured images of fluorescence from Rb atoms ionized by the e-beam (see Supplementary Material for details). While both signals are noisy, the measured centroid position variation matches within 12% between the two methods, indicating that the spatial coordinate systems agree with the two separate imaging systems. Similarly, we compare the total $e$beam current value, extracted from the polarization rotation measurements with that measured at the Faraday cup, located approximately 25 cm downstream, matching within 3% between the two methods.

Varying the electron beam energy between 10 to 20 keV yielded no significant changes in the profiles or quantities derived using the polarization rotation method.

From the fit, we also obtained a FWHM e-beam diameter of 1.70±0.54 mm. Although we are unable to independently verify the precise profiles of the electron beam, this value is noticeably broader than that obtained from the fluorescence fits – 0.89±0.04 mm FWHM. The uncertainty for these quantities are derived by considering the variance of the profile parameters of the datasets. We attribute this discrepancy between the widths to poor signal-to-noise ratio of the rotation signal, especially at the edges of the laser beam, where the laser power is low. The overall rotation signal was typically below 1 mrad, and thus strongly affected by the camera electronic noise. To improve the accuracy of the method, we need to enhance the magneto-optical atomic response by, for example, utilizing a more complex optical interrogation scheme to enhance atomic spin coherence and boost the magnetic re-

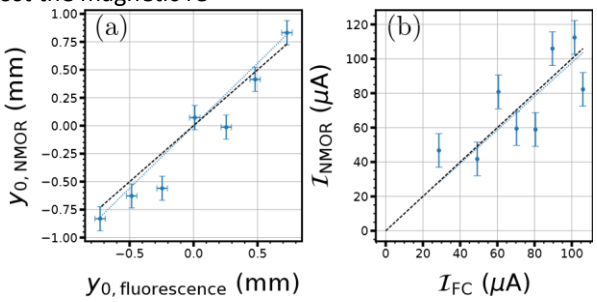

FIG. 3. (a) Comparison between the electron beam center position extracted from the polarization rotation measurement $y_{0,\mathrm{NMOR}}$ and from the electron-induced rubidium fluorescence images $y_{0,\mathrm{fluorescence}}$ with a regresssion of $y_{0,\mathrm{NMOR}} = (1.11 \pm 0.12)\, y_{0,\mathrm{fluorescence}}$. (b) Comparison between the total electron beam current calculated using the polarization rotation fits I_{NMOR} and measured directly using the Faraday cup I_{FC} of fit line $I_{\mathrm{NMOR}} = (0.97\pm0.08)\, I_{\mathrm{fluorescence}}$. The data is fit to a linear regression such that a perfect correspondence has a slope of 1. The dotted blue lines are linear fits of the data, while the black dashed lines represent a slope of 1, indicating matched correspondence between beam parameters.

sponse of atoms[19,20]. Also, using a low-noise CCD camera and pulsing the *e*-beam at faster rate will remove the dominant source of the technical noise and will boost the sensitivity by several order of magnitude, if limited by the laser shot noise (see Supplementary Material for details). Moreover, in this case, we may be able further improve the performance by using a non-classical (squeezed) optical field[21–26]. The ultimate spatial resolution of our method is diffraction limited and can potentially resolve details on the order of the probe laser wavelength $\lambda \approx 800$ nm.

Looking forward, higher sensitivity and spatial resolution could be achieved by employing advanced spectroscopic methods based on two or more lasers. For example, the 2D transverse current distribution can potentially be mapped out by 4-wave mixing, in which two intersecting probe lasers generate a third beam (imaged on a camera) that depends on the magnetic field in the crossing region[27]. Currently we are investigating 2- and 3-photon excitation to Rydberg states where we expect much higher sensitivity to the magnetic and electric fields from the *e*-beam due to their large Stark and Zeeman shifts[28,29]. Indeed, Rydberg states of ultracold atoms may have sufficient sensitivity for single particle detection[30].

In summary, thanks to nonlinear interaction with atomic spins, the light polarization rotates in a dilute alkali-metal vapor in the presence of the magnetic field produced by a passing charged particle beam. Taking advantage of this effect, we developed a non-invasive method for characterizing the transverse current distribution of an electron beam by that was obtained by mapping the nonlinear polarization rotation of a transverse probe laser crossing the *e*-beam. We have demonstrated this technique is capable to obtain the total current and transverse beam profile at 20 keV for *e*-beam currents between 30–110 μA. Since the *e*-beam is detected via its magnetic field, the scheme is insensitive to the beam energy, charged particle type and local electric fields associated with the beam.
We expect that this technique can be refined to meet the precision required for experiments at the frontier of nuclear and high-energy physics research.

SUPPLEMENTARY MATERIAL

See the supplementary material for detailed discussion of NMOR, sensitivity, and electron-induced rubidium fluorescence.

AUTHOR DECLARATIONS

Conflict of Interest

The authors have no conflicts to disclose.

Author Contributions

ACKNOWLEDGMENTS

This work is supported by U.S. DOE Contract No. DE-AC05-06OR23177, NSF award 2326736 and Jefferson Lab LDRD program. The collaboration thanks Jiahui Li and Cutter Fugett for their assistance in the early stages of the project.

Data Availability Statement

The data that support the findings of this study are available from the corresponding author upon reasonable request.

REFERENCES

[1]R. Bossart, J. Bosser, L. Burnod, E. d'Amico, G. Ferioli, J. Mann, F. Meot, and R. Coïsson, "Proton beam profile monitor using synchrotron light," in *11th International Conference on High-Energy Accelerators: Geneva, Switzerland, July 7–11, 1980*, edited by W. S. Newman (Birkhäuser Basel, Basel, 1980) pp. 470–475.

[2]S. Wang, D. Rubin, J. Conway, M. Palmer, D. Hartill, R. Campbell, and R. Holtzapple, "Visible-light beam size monitors using synchrotron radiation at cesr," Nuclear Instruments and Methods in Physics Research Section A: Accelerators, Spectrometers, Detectors and Associated Equipment 703, 80–90 (2013).

[3]W. Li, J. Yan, P. Liu, and Y. K. Wu, "Synchrotron radiation interferometry for beam size measurement at low current and in large dynamic range," Phys. Rev. Accel. Beams 25, 080702 (2022).

[4]T. Hofmann, G. Boorman, A. Bosco, S. Gibson, and F. Roncarolo, "A low-power laserwire profile monitor for h- beams: Design and experimental results," Nuclear Instruments and Methods in Physics Research Section A: Accelerators, Spectrometers, Detectors and Associated Equipment 903, 140–146 (2018).

[5]L. Corner, A. Aryshev, G. Blair, S. Boogert, P. Karataev, K. Kruchinin, L. Nevay, N. Terunuma, J. Urakawa, and R. Walczak, "Laserwire: A high resolution non-invasive beam profiling diagnostic," Nuclear Instruments and Methods in Physics Research Section A: Accelerators, Spectrometers, Detectors and Associated Equipment 740, 226–228 (2014), proceedings of the first European Advanced Accelerator Concepts Workshop 2013.

[6]R. Anne, Y. Georget, R. Hue, C. Tribouillard, and J. Luc Vignet, "A noninterceptive heavy ion beam profile monitor based on residual gas ionization," Nuclear Instruments and Methods in Physics Research Section A: Accelerators, Spectrometers, Detectors and Associated Equipment 329, 21–28 (1993).

[7]H. Sandberg, W. Bertsche, D. Bodart, S. Gibson, S. Jensen, S. Levasseur, K. Satou, G. Schneider, J. Storey, and R. Veness, "Commissioning of timepix3 based beam gas ionisation profile monitors for the CERN proton synchrotron." JACoW IBIC 2021, 172–175 (2021).

[8]A. Variola, R. Jung, and G. Ferioli, "Characterization of a nondestructive beam profile monitor using luminescent emission," Phys. Rev. ST Accel. Beams 10, 122801 (2007).

[9]A. Salehilashkajani, H. D. Zhang, M. Ady, N. Chritin, P. Forck, J. Glutting, O. R. Jones, R. Kersevan, N. Kumar, T. Lefevre, T. Marriott-Dodington, S. Mazzoni, I. Papazoglou, A. Rossi, G. Schneider, O. Sedlacek, S. Udrea, R. Veness, and C. P. Welsch, "A gas curtain beam profile monitor using beam induced

fluorescence for high intensity charged particle beams," Applied Physics Letters 120, 174101 (2022).

[10]H. Maesaka, H. Ego, S. Inoue, S. Matsubara, T. Ohshima, T. Shintake, and Y. Otake, "Sub-micron resolution rf cavity beam position monitor system at the sacla xfel facility," Nuclear Instruments and Methods in Physics Research Section A: Accelerators, Spectrometers, Detectors and Associated Equipment 696, 66–74 (2012).

[11]D. Budker and D. F. Jackson Kimball, eds., *Optical Magnetometry* (Cambridge University Press, Cambridge, 2013).

[12]A. Weis, G. Bison, and Z. D. Grujic, "Magnetic resonance based atomic´ magnetometers," in *High Sensitivity Magnetometers. Smart Sensors, Measurement and Instrumentation*, Vol. 19, edited by A. Grosz, M. Haji-Sheikh, and S. Mukhopadhyay (Springer, Cham, 2017) pp. 361–424.

[13]K. M. C. Fu, G. Z. Iwata, A. Wickenbrock, and D. Budker, "Sensitive magnetometry in challenging environments," AVS Quantum Science 2, 044702 (2020).

[14]We calculate a Bethe energy loss of 0.1 eV/m at a Rb density of 10^{12} atoms/cm^3 for 20 keV electrons. At 1 GeV, the energy loss is 0.04 eV/m.

[15]M. V. Balabas, T. Karaulanov, M. P. Ledbetter, and D. Budker, "Polarized alkali-metal vapor with minute-long transverse spin-relaxation time," Phys. Rev. Lett. 105, 070801 (2010).

[16]M. Rosner, D. Beck, P. Fierlinger, H. Filter, C. Klau, F. Kuchler, P. Rößner, M. Sturm, D. Wurm, and Z. Sun, "A highly drift-stable atomic magnetometer for fundamental physics experiments," Applied Physics Letters 120, 161102 (2022).

[17]V. G. Lucivero, W. Lee, N. Dural, and M. V. Romalis, "Femtotesla direct magnetic gradiometer using a single multipass cell," Physical Review Applied 15, 014004 (2021).

[18]D. Budker, W. Gawlik, D. F. Kimball, S. M. Rochester, V. V. Yashchuk, and A. Weis, "Resonant nonlinear magneto-optical effects in atoms," Rev. Mod. Phys. 74, 1153 (2002).

[19]F. Zhou, E. Y. Zhu, Y. L. Li, E. W. Hagley, and L. Deng, "Nanoteslalevel, shield-less, field-compensation-free, wave-mixing-enhanced bodytemperature atomic magnetometry for biomagnetism," (2018).

[20]C. J. Zhu, J. Guan, F. Zhou, E. Y. Zhu, and Y. Li, "Giant magneto-optical rotation effect in rubidium vapor measured with a low-cost detection system," OSA Continuum 4, 2527–2534 (2021).

[21]F. Wolfgramm, A. Cerè, F. A. Beduini, A. Predojevic, M. Koschorreck, and´ M. W. Mitchell, "Squeezed-light optical magnetometry," Physical Review Letters 105, 053601 (2010).

[22]T. Horrom, R. Singh, J. P. Dowling, and E. E. Mikhailov, "Quantumenhanced magnetometer with low-frequency squeezing," Physical Review A - Atomic, Molecular, and Optical Physics 86, 023803 (2012).

[23]N. Otterstrom, R. C. Pooser, and B. J. Lawrie, "Nonlinear optical magnetometry with accessible in situ optical squeezing," Opt. Lett. 39, 6533–6536 (2014).

[24]L. Bai, X. Wen, Y. Yang, L. Zhang, J. He, Y. Wang, and J. Wang, "Quantum-enhanced rubidium atomic magnetometer based on faraday rotation via 795 nm stokes operator squeezed light," Journal of Optics 23, 085202 (2021).

[25]J. Li and I. Novikova, "Improving sensitivity of an amplitude-modulated magneto-optical atomic magnetometer using squeezed light," J. Opt. Soc. Am. B 39, 2998–3003 (2022).

[26]S. Wu, G. Bao, J. Guo, J. Chen, W. Du, M. Shi, P. Yang, L. Chen, and W. Zhang, "Quantum magnetic gradiometer with entangled twin light beams," Science Advances 9, eadg1760 (2023).

[27]V. Boyer, C. F. McCormick, E. Arimondo, and P. D. Lett, "Ultraslow propagation of matched pulses by four-wave mixing in an atomic vapor," Phys. Rev. Lett. 99, 143601 (2007).

[28]N. Thaicharoen, K. R. Moore, D. A. Anderson, R. C. Powel, E. Peterson, and G. Raithel, "Electromagnetically induced transparency, absorption, and microwave-field sensing in a rb vapor cell," Phys. Rev. A 100, 063427 (2019).

[29]E. K. Dietsche, A. Larrouy, S. Haroche, J. M. Raimond, M. Brune, and S. Gleyzes, "High-sensitivity magnetometry with a single atom in a superposition of two circular rydberg states," Nature Phys. 15, 326 (2019).

[30]M. Jerkins, J. P. Klein, J. H. Majors, F. Robicheaux, and M. G. Raizen, "Using cold atoms to measure neutrino mass," New J. Phys. 12, 043022 (2010).